# Crystallization Kinetics of Poly(trimethylene terephthalate)

**JIEH-MING HUANG,[1,2] FENG-CHIH CHANG[2]**

[1] Department of Chemical Engineering, Van Nung Institute of Technology, Chung-Li, 32054 Taiwan

[2] Institute of Applied Chemistry, National Chiao-Tung University, Hsinchu, 30034 Taiwan

*Received 5 August 1999; revised 24 September 1999; accepted 11 January 2000*

**ABSTRACT:** The isothermal crystallization kinetics of poly(trimethylene terephthalate) (PTT) have been investigated using differential scanning calorimetry (DSC) and polarized light microscopy (PLM). Enthalpy data of exotherm from isothermal crystallization were analyzed using the Avrami theory. The average value of the Avrami exponent, $n$, is about 2.8. From the melt, PTT crystallizes according to a spherulite morphology. The spherulite growth rate and the overall crystallization rate depend on crystallization temperature. The increase in the spherulitic radius was examined by polarized light microscopy. Using values of transport parameters common to many polymers ($U^* =$ 1500 cal/mol, $T_\infty = T_g - 30$ °C) together with experimentally determined values of $T_m^0$ (248 °C) and $T_g$ (44 °C), the nucleation parameter, $k_g$, for PTT was determined. On the basis of secondary nucleation analyses, a transition between regimes III and II was found in the vicinity of 194 °C ($\Delta T \cong 54$ K). The ratio of $k_g$ of these two regimes is 2.1, which is very close to 2.0 as predicted by the Lauritzen–Hoffman theory. The lateral surface-free energy, $\sigma = 10.89$ erg/cm$^2$ and the fold surface-free energy, $\sigma_e = 56.64$ erg/cm$^2$ were determined. The latter leads to a work of chain-folding, $q = 4.80$ kcal/mol folds, which is comparable to PET and PBT previously reported. © 2000 John Wiley & Sons, Inc. J Polym Sci B: Polym Phys 38: 934–941, 2000

**Keywords:** poly(trimethylene terephthalate); crystallization kinetics; melting behavior; spherulitic growth rate; Avrami exponent

## INTRODUCTION

The family of linear aromatic polyesters, poly(ethylene terephthalate) (PET) and poly(butylene terephthalate) (PBT), have been widely studied. However, the poly(trimethylene terephthalate) (PTT) with three carbon atoms between ester groups has received considerably less attention. PTT is a relatively new polymeric material, which can be obtained by transesterification and polycondensation in the melt phase using trimethylene glycol and terephthalic acid with tetraisopropyl titanate as the catalyst.[1–3] The crystal structure of the PTT has been determined previously by electron diffraction and X-ray diffraction.[4] The dynamic mechanical relaxation and heat capacity of the PTT have also been studied.[2,5] Because PTT possesses good thermal and mechanical properties, it has been investigated recently as an engineering thermoplastic and as a matrix for fiber-reinforced composites.[6,7] In the polymer processing such as injection molding or extrusion, it is important to understand the crystallization kinetics of the polymer. Both the spherulite size and the degree of crystallinity influence the optical and mechanical properties of a polymer. It is well known that polymer crystallization involves two consecutive processes: the formation of nuclei and their subsequent growth. The study of the kinetics of crystallization is important for optimizing the process conditions and establishing the rela-

*Correspondence to:* F.-C. Chang (E-mail: changfc@cc.nctu.edu.tw)

Journal of Polymer Science: Part B: Polymer Physics, Vol. 38, 934–941 (2000)

tionship between thermal properties and structures of the polymer.

Three regimes of polymer crystallization have been proposed by Hoffman et al.[8,9] In regime I, at a high crystallization temperature, the physical meaning is associated with a process of crystallization where the rate of lateral spreading is greater than the rate of secondary nucleation. In regime II, at a higher supercooling, both rates are comparable. In regime III, at an even lower crystallization temperature, the rate of nucleation is substantially higher than that of the lateral spreading. The linear aromatic polyester poly(ethylene terephthalate) (PET) has been reported to have a regime II–regime III transition at about 165 °C with a slope ratio of 2.4.[10] The supercooling that occurred is quite large ($\Delta T$ = 115 K, based on $T_m^0$ = 280 °C), presuming a result of the stiffness of the PET. On the contrary, poly(butylene terephthalate) (PBT) with a flexible chain has been proposed to have a transition between regime II and III near 210 °C with a supercooling $\Delta T \cong 34$ K ($\Delta T$ based on $T_m^0$ = 244 °C).[11] As for the PTT, it has not been reported concerning the crystallization behaviors and regime transition phenomenon.

In this study we report our observations on the isothermal crystallization behavior of the PTT using DSC and PLM, then the data are analyzed by the Avrami equation and the nucleation theory. Finally, the surface-free energy and the work of chain-folding are calculated and compare these results with those from PET and PBT.

## EXPERIMENTAL

Poly(trimethylene terephthalate) (PTT) was obtained from the Shinkong Synthetic Fibers Co. (Taiwan) in the form of pellets. The intrinsic viscosity (I.V.) of the PTT in a 60:40 mixed solvent of phenol and tetrachloroethane at 25 °C was measured to be 0.80 dL/g. The weight and number-average molecular weights determined by gel permeation chromatography (GPC) were 46,300 g $mol^{-1}$ and 21,050 g $mol^{-1}$, respectively. The molecular weight distribution was 2.2.

The equilibrium melting point ($T_m^0$) measurement was carried out using a Perkin–Elmer DSC-7. The PTT sample was melted at 260 °C for 5 min under a nitrogen atmosphere to erase previous thermal histories. The sample was subsequently cooled at 300 °C/min to the desired crystallization temperature $T_c$. After crystallization for 24 h, the sample was immediately heated up from $T_c$ to 270 °C at a fixed heating rate of 10 °C/min. The peak temperature of the endotherm was considered as the melting point of the sample. For isothermal crystallization study, the sample was first heated to 260 °C and maintained at this temperature for 5 min, then cooled at a rate of 300 °C/min to the predetermined temperatures $T_c$. The exothermic curves as a function of time were recorded from 202 to 210 °C. In the study the isothermal crystallization kinetics by DSC, the weight fraction of crystallinity, $X(t)$, was calculated according to the following equation:[12–13]

$$\chi(t) = \frac{\int_0^t \frac{dH}{dt}\,dt}{\int_0^\infty \frac{dH}{dt}\,dt} \tag{1}$$

where the first integral is the heat generated at time $t$ and the second is the total heat generated up to the end of the crystallization process.

Measurement of the radius growth rate of PTT crystallites under isothermal crystallization was investigated using a polarized light microscopy (Leitz LABORLUX 12POLS) equipped with a heating stage (Linkam THMS-600), a temperature control system (Linkam TP-92), and a video recording system. Specimen was prepared by melting the PTT sample on a glass slide on a heating stage at 260 °C, followed by pressing of the melted sample with a piece of cover glass and maintained for 5 min at this temperature to remove any thermal history. Then the sample was rapidly quenched to the predetermined crystallization temperature. The subsequent growth of a particularly selected PTT spherulite was viewed between crossed polars and recorded by a video camera at appropriate time intervals. The spherulitic radius was measured directly from the video-record image. By plotting crystal radius versus time, the slope of the line or the spherulite growth rate $G$ at different temperatures (178–210 °C) can be obtained.

## RESULTS AND DISCUSSION

### Melting Behavior of PTT

DSC heating trace of the PTT after quenching from the melt and the subsequent cooling trace

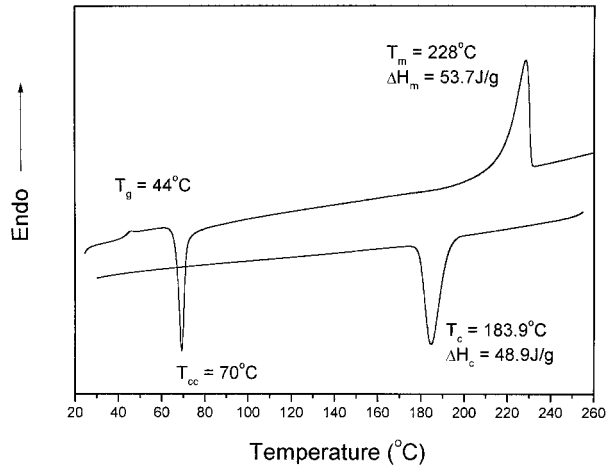


**Figure 1.** DSC heating trace after PTT quenching from the melt and the subsequent cooling trace. Heating and cooling rates are 10 °C.

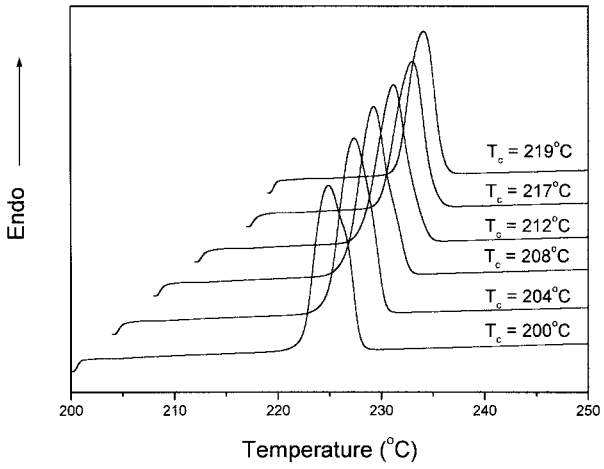


**Figure 3.** DSC heating curves for PTT crystallized at various temperatures for 24 h. Heating rate = 10 °C/min.

are shown in Figure 1. As seen in Figure 1, PTT is a semicrystalline polymer with a glass-transition temperature $T_g$ = 44 °C, melting temperature $T_m$ = 228 °C, and a cold crystallization temperature $T_{cc}$ = 70 °C. The measured glass-transition temperature $T_g$ = 44 °C is very close to $T_g$ = 45 °C previously reported by Gonzales et al.[2] and this value will be used to calculate the nucleation parameter $K_g$ in the following section. Figure 2 shows DSC heating traces at different heating rates for PTT isothermally crystallized at 210 °C for 1 h then quenched to room temperature. As the heating rate is increased, the low-temperature melting endotherm $T_m^1$ increases in size (relative to $T_m^2$) and its peak temperature, whereas

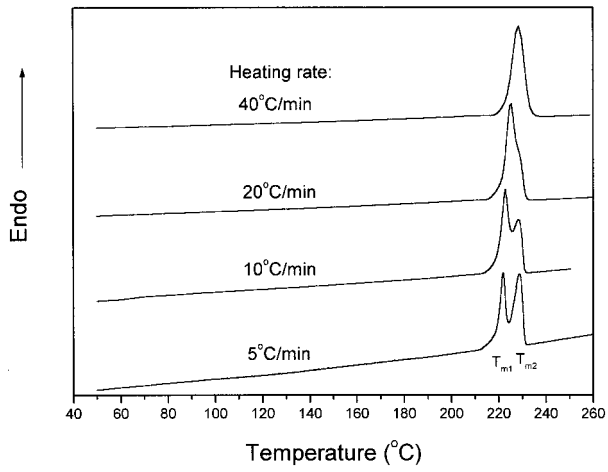


**Figure 2.** DSC traces of PTT crystallized at 210 °C for 1 h at various heating rates.

the high-temperature melting endotherm $T_m^2$ decreases in size and its peak temperature. However, the total heat of fusion does not change dramatically with different heating rates. A similar phenomenon was reported for PEEK isothermal crystallization at 220 °C.[14] When the heating rate is increased, the time allowed to recrystallization decreases and thus results in a smaller high-temperature melting endotherm and a larger low-temperature melting endotherm. From Figure 2 at the heating rate of 40 °C/min these two distinct melting endotherms appear to coalesce into a single endotherm because of a lower supercooling and less time allowed for recrystallization. It is noteworthy that the breadth of the coalesced endotherm is broader at this higher heating rate. From this result, the heating rate of 40 °C/min appears to be enough to minimize the reorganization during the heating in the DSC.

Figure 3 shows the typical melting behavior of PTT crystallized from 200 to 219 °C for 24 h. The equilibrium melting temperature, $T_m^0$, of the PTT can be determined by the Hoffman–Weeks equation,[15] using extrapolation of a plot of $T_m$ versus $T_c$ to $T_m = T_c$. The variation of the observed melting temperature with crystallization temperature $T_c$ is shown in Figure 4. In the range of $T_c$ explored, the $T_m$ of PTT increases almost linearly with $T_c$. The equilibrium melting temperature obtained by extrapolating to a value of $T_m^0$ = 248 °C, which is substantially higher than that previously reported by Pyda et al. (238 °C).[5] The $T_m^0$ (248 °C) obtained by this study is important in quantitative analysis of the crystallization behavior.

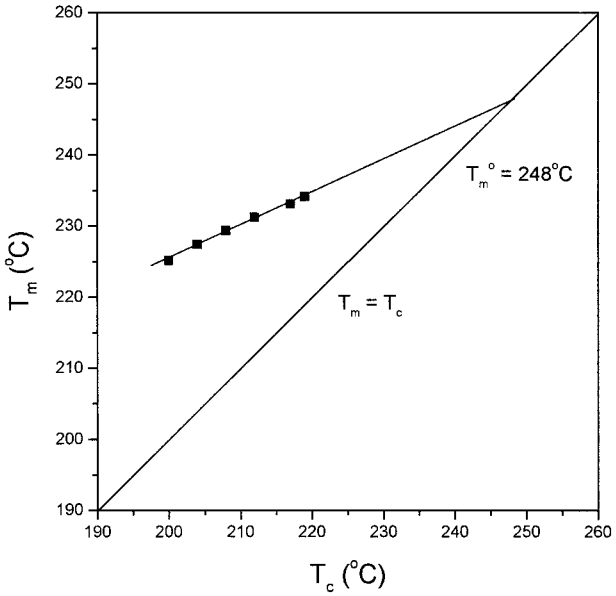


**Figure 4.** Hoffman–Weeks plot for isothermally crystallized PTT (24-h crystallization).

## Isothermal Crystallization Behavior of PTT

Figure 5 shows the exothermic traces for PTT samples isothermal crystallization from 202 to 210 °C. The crystallization process finishes in less than 40 min. As would be expected, a sample with higher crystallization temperature requires a longer time to complete crystallization. By following the Avrami treatment, the relative crystallinity as a function of crystallization time is plotted in Figure 6. From these curves, the half-time of crystallization $t_{1/2}$ defined as the time required for half of the final crystallinity to develop, was obtained. The variation of $t_{1/2}$ and $\log(t_{1/2})^{-1}$ with crystallization temperature $T_c$ is shown in Figure 7, where the $t_{1/2}$ is strongly dependent on the crystallization temperature. From the relation between $\log(t_{1/2})^{-1}$ and $T_c$, the plot exhibits a discontinuity around $T_c$ = 195 °C, indicating that two crystallization processes are involved in the $T_c$ region from 180 to 214 °C. An important observation is that this plot resembles the result in spherulite growth rate determined from the polarized light microscopy (in latter section). This in turn is related to changes in regimes.[16]

The isothermal crystallization kinetics of PTT were analyzed on the basis of the Avrami equation:[17,18]

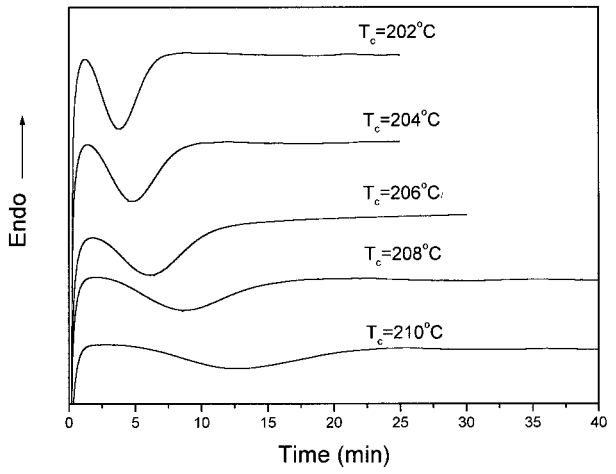


**Figure 5.** Isothermograms of PTT at the indicated $T_c$ on each curve.

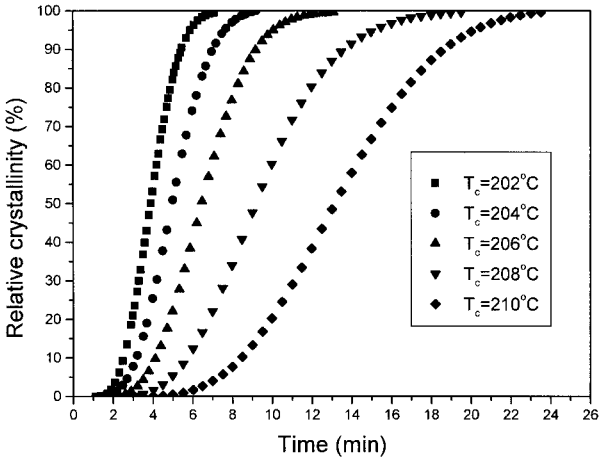


**Figure 6.** Relative crystallinity versus time for PTT crystallized at different crystallization temperatures.

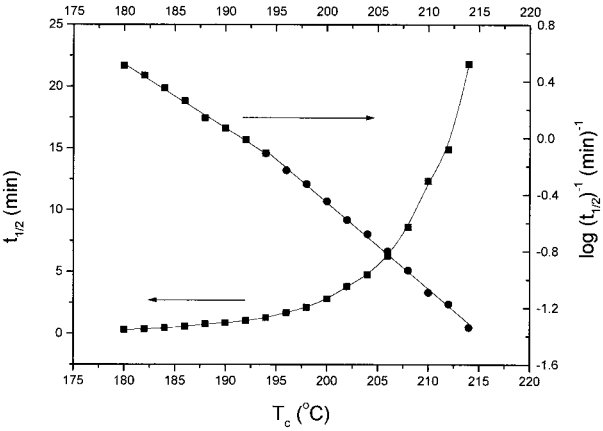


**Figure 7.** Half-time of crystallization $t_{1/2}$ and $\log(t_{1/2})^{-1}$ as a function of $T_c$ for PTT crystallized from the melt state.

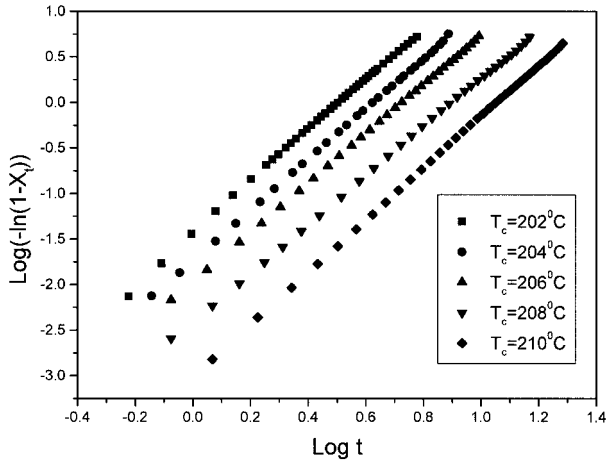


**Figure 8.** Avrami plots for PTT at different crystallization temperatures.

$$\log[-\ln(1 - X_t)] = \log k + n \log(t) \qquad (2)$$

where $X(t)$ is the weight fraction of crystallinity, $n$ is the Avrami exponent, $k$ is the overall kinetic rate constant and $t$ is the time of crystallization. Both $k$ and $n$ depend on the mechanism of the nucleation as well as the growth geometry. The value of $n$ is usually an integer between 1 and 4 for different crystallization mechanisms. It has also been observed that $n$ is a fraction due to the secondary crystallization or the crystal perfection. Indeed, for spherulitic growth and athermal nucleation $n$ is expected to be 3. In the case of thermal nucleation, it is expected to be 4. The double logarithmic plots of the Avrami analysis for PTT at different crystallization temperatures are shown in Figure 8. The experimental data appear to fit extremely well with the Avrami equation, plots of log $[-\ln(1\text{-}X_t)]$ versus log $(t)$ at different $T_c$ all result in linear relationship. From the slope and intercept of the Avrami plot, the Avrami exponent $n$ and the overall rate constant $k$ are obtained and tabulated in Table I. From the Table, the half-time of crystallization $t_{1/2}$ decreases exponentially with decreasing crystallization temperature, indicating that the rate of crystallization is faster when the supercooling is larger. The overall rate constant $k$ is extremely sensitive to temperature, which determines both the nucleation and the growth processes. Furthermore, the overall rate constant is faster when the crystallization temperature is decreased, which is similar to the result from the polarized light microscopy observation. The average value of the $n$ determined in each crystallization temperature is about 2.8, indicating that both the nucleation and the growth mechanism are the same in the crystallization temperature range investigated. This value of $n$ is slightly lower than the theoretical value of 3.0 predicted for instantaneous nucleation with spherulitic growth geometry. Combining the observation from DSC and the later polarized light microscopy, it seems to be in regime II crystallization by assuming the competition between secondary nucleation and lateral lamellar growth.

In comparison with PTT, the isothermal crystallization behaviors of PET and PBT have drawn much more attention. For the PET, the Avrami exponent $n$ ranging from $2 \sim 4$ has been reported, depending on the molecular weight, chemical purity, melt condition, and crystallization temperature.[13,19–21] For example, the overall crystallization kinetics change from slow crystallization with an Avrami exponent $n = 2$ at 90–160 °C to $n = 3$ in the faster crystallization, and finally approaches $n = 4$ above 230 °C where the crystallization rate is slow again. As for the PBT, the Avrami exponent $n = 2.6$–$2.8$ has been reported, and the melt crystallizes faster than the PET under same supercooling condition.[13,22]

## Growth Rate Parameters in Crystallization of PTT

Figure 9 shows the polarized light micrographs of PTT isothermally crystallized from the melt at 204 °C for various time intervals. It is clear that the crystal grows as spherulite morphology. The positive Maltese cross pattern is evident, indicating along or perpendicular to orientation of the crystalline molecular axis with respect to the spherulitic radius.[23,24] The dimensions of the crystallites are very sensitive to the crystallization temperature and time. Figure 10 gives plots of the spherulite radius versus time for different crystallization temperatures. The solid lines represent the best least-squares fit to the data. It is

**Table I.** Isothermal Crystallization Parameters of PTT

| $T_c$ (°C) | $n$ | $k$ | $t_{1/2}$ (min) |
|---|---|---|---|
| 202 | 2.81 | $33.7 \times 10^{-3}$ | 2.90 |
| 204 | 2.77 | $18.4 \times 10^{-3}$ | 3.69 |
| 206 | 2.72 | $10.8 \times 10^{-3}$ | 4.65 |
| 208 | 2.70 | $3.9 \times 10^{-3}$ | 6.84 |
| 210 | 2.84 | $1.0 \times 10^{-3}$ | 9.87 |

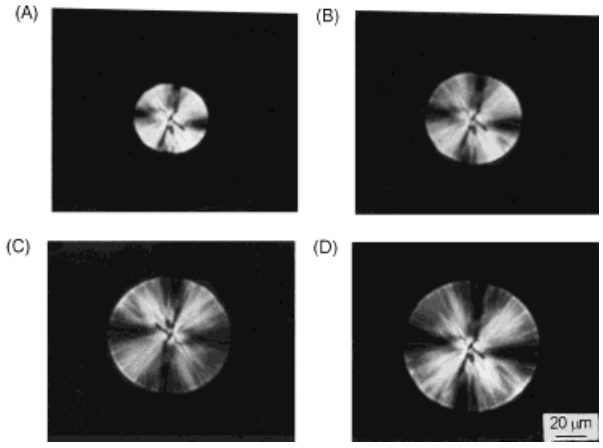


**Figure 9.** Polarized light micrographs of PTT isothermally crystallized at 204 °C for various times: (A) 93 s; (B) 120 s; (C) 153 s; (D) 170 s.

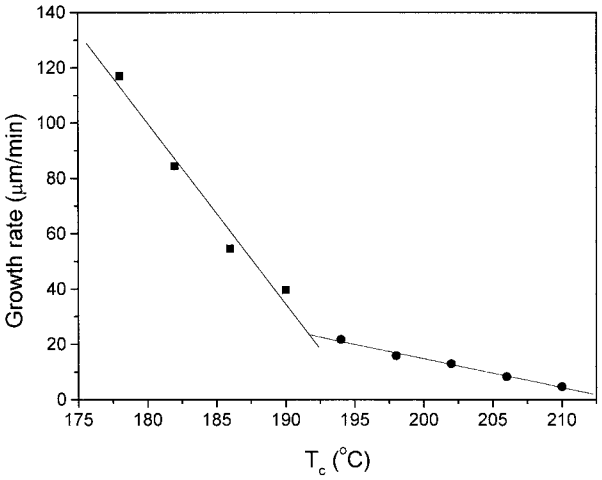


**Figure 11.** Spherulite growth rate as a function of crystallization temperature.

clear that there is a linear increase in the radius with time until the spherulites impinge on each other. It was also observed that the induction time for nucleation becomes longer at higher crystallization temperature. From the slopes of the straight lines at various crystallization temperatures, the spherulite growth rate $G$ has been calculated ranging from 117.0 to 4.7 $\mu$m/min. The plot of $G$ as a function of crystallization temperature is displayed in Figure 11. In the range of crystallization temperature studied, $G$ decreased dramatically as the crystallization temperature is increased. Furthermore, the plot seems can be fitted by two straight lines, and a temperature break, $T_{\text{break}}$ at about 192 °C is observed. The two different sections of the curve may be taken as an indication of change in regime crystallization. It is interesting to compare this result with Figure 7 determined by DSC where also has a $T_{\text{break}}$ at 195 °C.

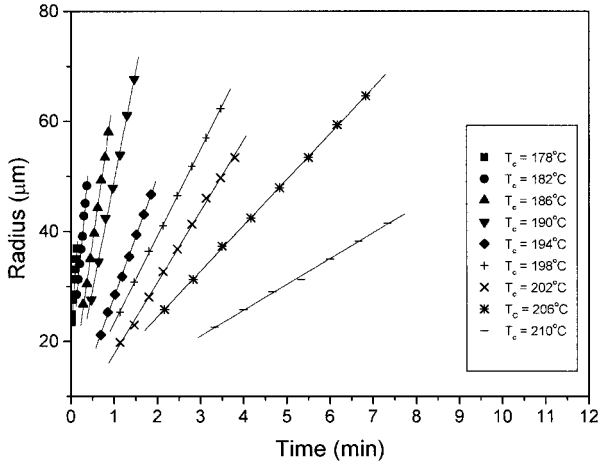


**Figure 10.** Radius of spherulite as a function of time for different crystallization temperatures.

The general expression for the growth rate of a linear polymer crystal with folded chains is given by:[8]

$$G = G_0 \exp\left(\frac{-U^*}{R(T_c - T_\infty)}\right) \exp\left(\frac{-K_g}{T_c \Delta T f}\right) \qquad (3)$$

where $G_0$ is the front factor; $U^*$ is the activation energy for the segment diffusion to the site of crystallization; $R$ is the gas constant; $T_\infty$ is the hypothetical temperature below which all viscous flow ceases; $T_\infty = T_g - 30$ °C; $K_g$ is the nucleation parameter; $\Delta T$ is the degree of supercooling defined by $T_m^0 - T_c$; and $f$ is a correction factor given as $2T_c/(T_m^0 + T_c)$. Growth rates at a relatively low degree of supercooling is well known to be relatively insensitive to the values of $U^*$ and $T_\infty$ employed in eq 3, and the "universal" values of $U^*$ = 1500 cal/mol and $T_\infty = T_g - 30$ °C were used in all calculations. The nucleation parameter $K_g$ is given by:

$$K_g = \frac{nb\sigma\sigma_e T_m^0}{\Delta h_f k_B} \qquad (4)$$

where $b$ is the thickness of a monomolecular layer; $\sigma$ is the lateral surface-free energy; $\sigma_e$ is the fold surface-free energy; $\Delta h_f$ is the heat of fusion per unit volume; $T_m^0$ is the equilibrium melting point; and $k_B$ is the Boltzmann's constant. Typi-

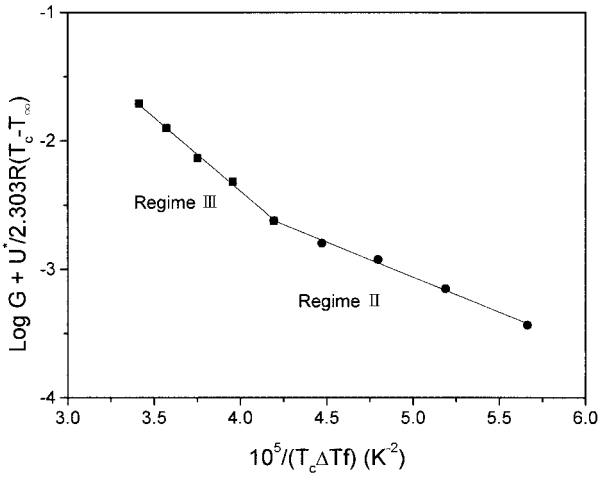


**Figure 12.** Plot of log $G + U^*/2.303R(T_c - T_\infty)$ as a function of $1/T_c\Delta Tf$.

cally the value of $n = 4$ in regime I or III and $n = 2$ in regime II have been employed. It is often most convenient to rearrange eq 3 as:

$$\log G + \frac{U^*}{2.303R(T_c - T_\infty)} = \log G_0 - \frac{K_g}{2.303T_c(\Delta T)f} \quad (5)$$

and view the growth rate data in the form of a plot of the left-hand side of eq 5 versus $1/T_c(\Delta T)f$, with a slope $= -K_g$. Figure 12 shows the growth rate data for PTT plotted according to indications of eq 5. On the basis of secondary nucleation analyses, a transition between regime III and II is found in the vicinity of 194 °C ($\Delta T \cong 54$ K). This regime III/II transition temperature of PTT is higher than that of PET (165 °C) but lower than that of PBT (210 °C).[10,11] In the calculation, $T_g$ of 44 °C and $T_m^0$ of 248 °C were used for PTT as determined by DSC experiments. It appears reasonable to fit the experimental data with two straight lines, and from the slopes obtain the $K_{g(III)} = 3.02 \times 10^5$, $K_{g(II)} = 1.45 \times 10^5$, respectively. The ratio of slope between $K_{g(III)}$ and $K_{g(II)}$ is 2.1, which is very close to 2.0 as predicted by the Lauritzen–Hoffman theory.

The derived $K_g$ can be used to calculate $\sigma_e$ and the work of chain-folding, $q$, for the PTT. Using the layer thickness $b = 6.266$ Å,[4] $T_m^0 = 248$ °C and $\Delta h_f = 145.6$ J/g,[5] we derived the $\sigma\sigma_e = 616.7 \times 10^{-6}$ J$^2$/m$^4$. The lateral surface-free energy $\sigma$ may be estimated by the Thomas–Stavely relationship:[8]

$$\sigma = \alpha \cdot \Delta h_f \cdot (ab)^{1/2} \quad (6)$$

where $a$ is the molecular width, $\alpha$ is an empirical constant, and $\alpha$ is usually assumed to be ~0.1. Taking $\alpha = 0.1$, $\sigma$ can be calculated to be 10.89 erg/cm$^2$ from eq 6, and using the experimental $K_g$ leads to the fold surface-free energy $\sigma_e = 56.64$ erg/cm$^2$. The work of chain-folding, $q$, has been found to be one parameter most closely correlated with molecular structure, and probably the most important contribution to its relative magnitude is thought to be the inherent stiffness of the chain itself.[8,11] The work of chain-folding can be derived from $\sigma_e$ by the following relationship:

$$q = 2ab\sigma_e \quad (7)$$

where $ab$ is the molecular cross-sectional area, and for PTT is 0.29 nm$^2$. This value of $q$ calculated from eq 7 is 4.80 kcal/mol folds. It is worth noting that the value of $q$ is fairly comparable to other polymers. The values of $\sigma_e = 56.64$ erg/cm$^2$ and $q = 4.80$ kcal/mol of folds estimated for PTT are reasonable and fit into the range of values for other polymers. For comparison, the kinetic parameters of PET and PBT are also listed in Table II. It is well known that PET crystallizes more slowly than PBT. As seen in Table II , the work required to form a PBT fold is roughly half of that of PET, and hence chain-folding is less hindered to crystallize for PBT. From Table II, we can conclude that PTT crystallizes faster than PET

**Table II.** Comparison of Surface-Free Energies and Work of Chain-Folding for PET, PTT, and PBT

| Polymer | $T_g$ (°C) | $K_{g(II)} \times 10^{-5}$ (deg$^2$) | $\sigma$ (erg/cm$^2$) | $\sigma_e$ (erg/cm$^2$) | $q$, kcal/ (mol of folds) | Source |
|---|---|---|---|---|---|---|
| PET | 75 | 2.81 | 10.6 | 140 | 10.0 | Ref. 25 |
| PTT | 46 | 1.45 | 10.89 | 56.64 | 4.8 | This work |
| PBT | 42 | 0.53 | 8.8 | 57–75 | 3–5 | Ref. 11 |

because the work of chain-folding for PTT is lower than that of PET. This relatively large difference in $q$ is related to the longer flexible segments [i.e., $(CH_2)_3$ versus $(CH_2)_2$] in the PTT repeat unit. From a scientific viewpoint, thermodynamic information from PTT coupled with corresponding data from poly(ethylene terephthalate) (PET) and poly(butylene terephthalate) (PBT) makes knowledge on this polyester family more complete.

## CONCLUSIONS

In this study, we investigated the crystallization kinetics of PTT by means of differential scanning calorimetry and polarized light microscopy. The PTT specimen shows an Avrami exponent $n = 2.8$ in the isothermal crystallization temperatures explored. Combining the observation from DSC and polarized light microscopy, it seems to be in regime II crystallization, assuming the competition between secondary nucleation and lateral lamellar growth. The equilibrium melting temperature was determined and found at 248 °C. Using $U^* = 1500$ cal/mol together with the determined $T_g$ and $T_m^0$, the nucleation parameter $K_g$ was determined. A transition between regime III and II was found near 194 °C. Furthermore, the relation between $\log(t_{1/2})^{-1}$ and $T_c$ determined from DSC also shows the $T_{\text{break}}$ at 195 °C, implying the change in regimes. The surface-free energies $\sigma = 10.89$ erg/cm$^2$ and $\sigma_e = 56.64$ erg/cm$^2$ were estimated. The work of chain-folding ($q = 4.80$ kcal/mol folds) derived from $\sigma_e$, is close to the PBT but substantially lower than that of the PET. Therefore, we can conclude that in the family of the linear aromatic polyesters, PBT and PTT are more flexible than that of PET.

The financial support by the National Science Council under grant NSC87-2216-E-009-006 is greatly appreciated. The authors are also indebted to Shinkong Synthetic Fibres Co. for supporting poly(trimethylene terephthalate) samples.

## REFERENCES AND NOTES

1. Ng, T. H.; Williams, H. L. Makromol Chem 1981, 182, 3323.
2. Gonzalez, C. C.; Perena, J. M.; Bello, A. J Polym Sci Polym Phys Ed 1988, 26, 1397.
3. Imamura, T.; Sato, T.; Matsumoto, T. Jpn Patent 08,232,117, 1996.
4. Peres, S.; Suzie, P. D.; Revol, J. F.; Brisse, F. Polymer 1979, 20, 419.
5. Pyda, M.; Boller, A.; Grebowicz, J.; Chuah, H.; Lebedev, V.; Wunderlich, B. J Polym Sci Polym Phys Ed 1998, 36, 2499.
6. Dangayach, K.; Chuah, H.; Gergen, W.; Dalton, P.; Smith, F. Plastics—Saving Planet Earth. Proceedings of the 55th ANTEC Conference, 1997; p 2097.
7. Tsumashima, K.; Suzuki, M. Jpn Patent 08,104,763, 1996.
8. Hoffman, J. D.; Davis, G. T.; Lauritzen Jr., J. I. In Treatise on Solid-State Chemistry; Hannay, N. B., Ed.; Plenum Press: New York, 1976; Vol. 3.
9. Clark, E. J.; Hoffman, J. D. Macromolecules 1984, 17, 878.
10. Phillips, P. J.; Tseng, H. T. Macromolecules 1989, 22, 1649.
11. Runt, J.; Miley, D. M.; Zhang, X.; Gallagher, K. P.; McFeaters, K.; Fishburn, J. Macromolecules 1992, 25, 1929.
12. Mancarella, C.; Martucelli, E. Polymer 1977, 13, 407.
13. Wunderlich, B. Macromolecular Physics; Academic Press: New York, 1976.
14. Lee, Y.; Porter, R. S. Macromolecules 1987, 20, 1336.
15. Hoffman, J. D.; Weeks, J. J. J Chem Phys 1965, 42, 4301.
16. Mandelkern, L.; Fatou, J. G.; Marco, C. Polymer 1990, 31, 1685.
17. Avrami, M. J Chem Phys 1939, 8, 212.
18. Avrami, M. J Chem Phys 1941, 9, 177.
19. Ravindranath, K.; Jog, J. P. J Appl Polym Sci 1993, 49, 1395.
20. Kim, S. C.; Kim, S. P. Polym Eng Sci 1993, 33, 83.
21. Lin, C. C.; Ou, C. F. J Appl Polym Sci 1994, 54, 1223.
22. Gilbert, M.; Hybart, F. J. Polymer 1972, 13, 327.
23. Samuels, R. J. J Polym Sci Polym Phys Ed 1971, 9, 2165.
24. Haudin, J. M. Optical Properties of Polymers; Elsevier: London, 1986.
25. van Antwerpen, F.; van Krevelen, D. W. J Polym Sci Polym Phys Ed 1972, 10, 2423.